

# Enhanced Photocatalytic and Self-Cleaning Performance of Anatase Titanium dioxide Nanoparticles Synthesized via a Modified Sol-Gel Method

Hadeel Salih Mahdi<sup>1</sup> and Mawlood Maajal Ali<sup>2</sup>

<sup>1</sup>Department of Science, College of Basic Education, University of Misan, 62001 Misan, Iraq

<sup>2</sup>Department of Medical Physics, College of Applied Sciences - Heet, University of Anbar, 31001 Anbar, Iraq  
hadeel.salih@uomisan.edu.iq, mawloodmali@uoanbar.edu.iq

**Keywords:** Titanium Dioxide Nanoparticles, Sol–Gel Synthesis, Photocatalysis, Self-Cleaning.

**Abstract:** Titanium dioxide nanoparticles (TiO<sub>2</sub>NPs) had been synthesized using a modified sol-gel technique as well as characterized through UV-Visible spectroscopy, scanning electron microscopy (SEM), X-ray diffraction (XRD) and Fourier transform infrared (FTIR) Spectroscopy, with a band gap of 3.12eV and a pure anatase phase. TiO<sub>2</sub>NPs had a significant UV absorption as well as an average particle size of approximately 80nm. The objective of this research was to investigate the photocatalytic activity and superhydrophilic behavior of anatase TiO<sub>2</sub>NPs. According to first-order kinetics, photocatalytic performance has been assessed by evaluating the degradation of organic contaminants under UV irradiation, which resulted in up to 88% removal in 60 minutes. Furthermore, the water contact angle dropped from 70° to less than 5°, demonstrating the TiO<sub>2</sub>NPs' strong UV-induced superhydrophilicity and demonstrating their capacity for self-cleaning. These TiO<sub>2</sub>NPs appear to be promising options for environmental applications, such as wastewater treatment and self-cleaning coatings in solar panels and building facades, due to their high photocatalytic efficiency as well as superhydrophilic behavior.

## 1 INTRODUCTION

Over recent years, the investigation into environmental protection from pollution has become a crucial research priority. Industrial waste discharged into water bodies such as rivers and lakes is a significant contributor to environmental contamination, posing severe risks to the food chain and causing harmful effects on plants and animals. Many of these pollutants are organic molecules, which can be degraded through photocatalysis, a promising green technology for environmental remediation [1], [2]. The use of semiconductor nanostructures in photocatalytic oxidation has drawn interest for treating wastewater because of its effectiveness in mineralizing harmful organic compounds into harmless end products, like H<sub>2</sub>O and CO<sub>2</sub>. The photocatalytic activity of several semiconductor nanomaterials, including CuO, ZnO, TiO<sub>2</sub>, CdS, ZnS, and iron oxides, was studied [3]-[5]. With a band gap of roughly 3.2eV, TiO<sub>2</sub> is seen to be the most promising because of its special qualities, which include low toxicity, strong

photoactivity, high refractive index, great chemical stability, and transparency in the visible spectrum [6]-[8]. There are 3 primary crystalline phases of TiO<sub>2</sub>: rutile, anatase, and brookite. The anatase phase usually has higher photocatalytic efficacy than rutile phase because of its lower electron-hole recombination rate [9], [10]. Under UV irradiation, electrons are excited from valence band (VB) to conduction band (CB), which leads to electron-hole pairs, which is the basis of the photocatalytic mechanism. The hydroxyl (•OH) and superoxide (•O<sub>2</sub><sup>-</sup>) radicals, which are extremely reactive species that can degrade organic pollutants, are created when such charge carriers move to the catalyst surface and react with molecules of H<sub>2</sub>O and O<sub>2</sub> [11]. TiO<sub>2</sub> NPs were widely used in self-cleaning surfaces, in which the material's superhydrophilicity and photocatalytic degradation regarding organic contaminants allow dirt and organic matter to be readily removed with water [12], [13].

Self-cleaning coatings, glass panels, and fabrics utilizing TiO<sub>2</sub> NPs have demonstrated significant potential in reducing maintenance costs, improving

environmental cleanliness, and promoting sustainable building technologies. Various synthesis methods like sol-gel [14], chemical precipitation [15], microwave irradiation [16], and hydrothermal processes [17] have been reported to tailor TiO<sub>2</sub> morphology (nanoparticles, nanorods, nanocubes, nanowires) and optimize photocatalytic efficiency. Comparative studies show that anatase-phase TiO<sub>2</sub> NPs prepared via sol-gel methods often exhibit higher photocatalytic degradation rates than those prepared by chemical precipitation or hydrothermal synthesis, due to smaller particle size and larger surface area [18], [19]. Additionally, doped or composite TiO<sub>2</sub> systems (e.g., TiO<sub>2</sub>-ZnO, TiO<sub>2</sub>-Ag) have been shown to improve the photocatalytic activity and extend absorption spectrum into visible region, further improving self-cleaning and water-treatment performance [20], [21].

In this study, synthesize anatase-phase TiO<sub>2</sub> nanoparticles using a modified sol-gel method to obtain high crystallinity and controlled particle size. The study aimed to first characterize TiO<sub>2</sub> for its photocatalytic activity in degrading organic contaminants (methylene blue dye) upon exposure to UV light, and also to monitor the UV light-induced superhydrophilicity for potential self-cleaning applications. This approach highlights the utility of functionalizing TiO<sub>2</sub> nanostructures based on sol-gel synthesis to improve their functional properties to achieve an environmentally beneficial application for environmental remediation and surface applications sustainably.

## 2 MATERIALS AND INSTRUMENTS

### 2.1 Materials

Titanium isopropoxide (TTIP, Ti[OCH(CH<sub>3</sub>)<sub>2</sub>]<sub>4</sub>, Sigma-Aldrich, USA) and nitric acid (HNO<sub>3</sub>, 65%, Merck, Germany). Isopropanol (C<sub>3</sub>H<sub>8</sub>O, 99.5%, Merck, Germany), Methylene blue dye (Loba Chemie, India) and deionized water were used as solvents. All chemicals were of analytical grade.

### 2.2 Synthesis of TiO<sub>2</sub> Nanoparticles

The method of *M. M. Ahmad et al.* [22] was modified and TiO<sub>2</sub> nanostructures were synthesized utilizing this modified technique. The titanium isopropoxide (TTIP, 0.4 M) and nitric acid (HNO<sub>3</sub>) were used as received and without purification. A mixture of 10.0

mL isopropanol and 12.0 mL deionized water was continuously stirred at 80 °C in a round-bottom flask for a total volume of 22 mL. The TTIP solution was then added dropwise under intense stirring for 20 mL of 0.4 M. One hour later, 0.8 mL concentrated nitric acid diluted with deionized water was added to the mixture, resulting in a viscous sol-gel. The mixture was further stirred for 6 hr at 60 °C, after which it was heated to 300 °C for two hours. The product was a nanocrystalline TiO<sub>2</sub> powder, which was ground to a fine powder using a mortar and pestle.

### 2.3 Preparation of Anatase TiO<sub>2</sub> Thin Films

Anatase TiO<sub>2</sub> thin films were prepared for contact angle measurements by depositing a sol-gel-derived TiO<sub>2</sub> solution onto clean glass substrates using the dip-coating method. The coated substrates were dried at moderate temperature and subsequently annealed at 300–350 °C to achieve crystallization in the anatase phase, forming uniform films suitable for evaluating UV-induced superhydrophilicity using a contact angle goniometer.

### 2.4 Characterization Techniques

The synthesized TiO<sub>2</sub> nanoparticles (TiO<sub>2</sub> NPs) were comprehensively characterised using multiple techniques. Optical properties were analysed using UV-visible spectroscopy (Shimadzu UV-1900, Japan) over the range of 190–800 nm. Structural features were examined by X-ray diffraction (XRD, Philips) with data collected over a 2θ range of 10°–80°. The morphology and surface characteristics of the nanoparticles were observed using scanning electron microscopy (SEM, Inspect F-50). Functional groups in both the nanoparticles and the plant extract were identified via Fourier Transform Infrared Spectroscopy (FTIR 7800A, UK).

Additionally, the water contact angle of the TiO<sub>2</sub> nanoparticle surfaces was measured using a Contact Angle Goniometer via the sessile drop method with a 4 μL deionised water droplet. The static contact angle was automatically determined by the instrument's software, and the reported values represent the average of five measurements across the sample surface.

## 3 RESULTS AND DISCUSSIONS

Figure 1 displays the room temperature XRD patterns of TiO<sub>2</sub>NPs sample. With a crystal structure that

matches the anatase phase, the patterns show clear Bragg peaks, demonstrating that TiO<sub>2</sub> is nanocrystalline. The anatase phase of TiO<sub>2</sub>NPs is well characterized by the diffraction peaks seen at 2θ values of 25.1°, 37°, 37.9°, 38.5°, 48.2°, 54.0°, 55.2°, 62.8°, 68.7°, 70.1°, and 75.1°, which may be indexed to the crystal planes (101), (103), (004), (112), (200), (105), (211), (204), (116), (220), and (215), respectively. Excellent agreement has been found between such results and the standard JCPDS card (No. 21-1272). The effective production of the anatase crystalline phase without visible impurities or secondary phases is indicated by the locations of all diffraction peaks matching the reference data.

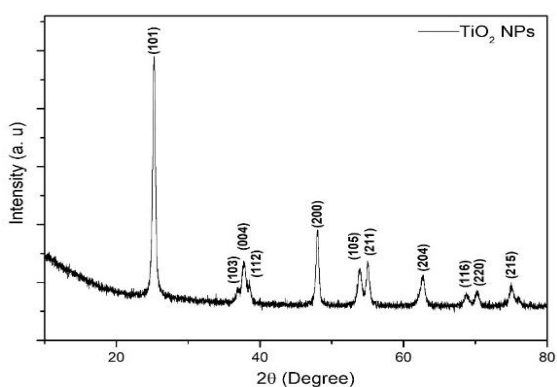


Figure 1: XRD pattern of the TiO<sub>2</sub>NPs.

The crystal size (D) of titanium dioxide nanostructures is estimated using Debye-Scherrer [23]:

$$D = \frac{k\lambda}{\beta \cos\theta} \tag{1}$$

where: (K) is a constant that is equal to 0.90, (λ) is the wavelength of X-rays used, 0.15406nm, (β) is the FWHM, and θ is the Bragg angle of diffraction. The crystal size has been found to be about 78nm as shown in Table 1.

Table 1: Estimated crystallite size.

Plane (hkl)	2θ (°)	β (FWHM)	D (nm)
(101)	25.1	0.104	78

The FTIR spectrum of the synthesized TiO<sub>2</sub> nanoparticles confirms the formation of the anatase phase as shown in Figure 2. A broad band at 3416 cm<sup>-1</sup> corresponds to O–H stretching from surface hydroxyls and adsorbed water, while the band near 1641 cm<sup>-1</sup> arises from H–O–H bending vibrations. Weak features around 1105 cm<sup>-1</sup> indicate minor residual organics. Strong absorption bands at

approximately 636 and 468 cm<sup>-1</sup> are characteristic of Ti–O–Ti lattice vibrations, confirming the crystalline anatase structure [24], [25]. The absence of other impurity peaks suggests the high purity of the obtained TiO<sub>2</sub> nanoparticles [26].

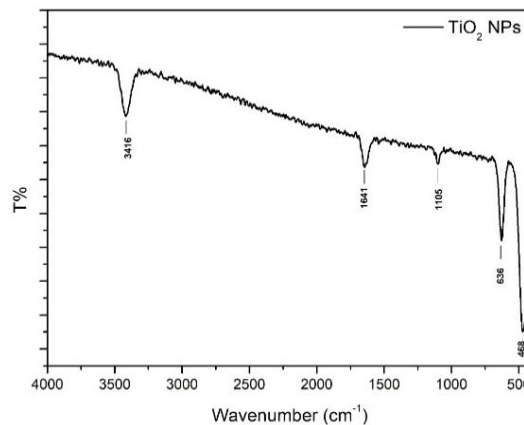


Figure 2: FTIR spectrum of the TiO<sub>2</sub>NPs.

SEM was used in order to analyze the surface morphology of nanostructures from a top view. The images revealed that the nanoparticles exhibit a predominantly spherical shape with a uniform size distribution. Agglomeration of nanoparticles was observed, leading to the formation of peak-like structures as a result of surface energy minimization and van der Waals interactions. The average particle size that had been estimated from SEM images was approximately 80 nm Figure 3. This size is almost close to the crystallite size that had been calculated from XRD with the use of Scherrer equation. The close agreement between particle and crystallite sizes confirms the high crystallinity of the synthesized TiO<sub>2</sub> nanoparticles, which is critical for enhanced photocatalytic efficiency by minimizing grain boundary defects and promoting effective charge carrier separation [27].

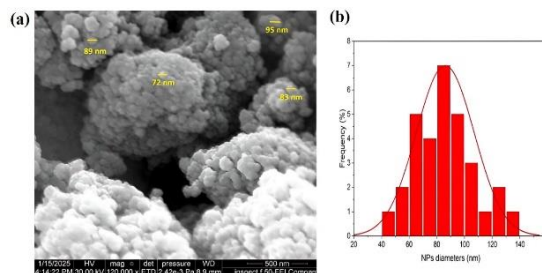


Figure 3: (a) SEM image and (b) EDX spectrum of TiO<sub>2</sub> nanoparticles.

The optical properties of the TiO<sub>2</sub> nanoparticles have been investigated. The absorbance spectrum, depicted in Figure 4, was recorded over the wavelength range of 190nm to 800nm. A distinct absorption peak was observed at approximately 325 nm, indicating strong absorbance in the ultraviolet (UV) region, which is characteristic of anatase phase of TiO<sub>2</sub> [28]. As illustrated in Figure 4, Tauc plot approach was utilized in order to determine the optical band gap. The TiO<sub>2</sub> NPs' computed band gap energy was 3.12 eV, which is marginally less than the 3.2 eV value regarding the bulk anatase TiO<sub>2</sub>. This decrease is explained by surface defect states as well as quantum size effects, which are frequently seen in NPs and affect their electronic structure and optical transitions [29]. Through improving the use of UV light, this type of band gap tuning helps to increase photocatalytic activity. The effective production of TiO<sub>2</sub> NPs with desired optical properties for photocatalytic as well as self-cleaning applications is confirmed by UV-Vis absorbance measurements, which show a good correlation with the crystalline nature and particle size obtained from SEM and XRD analyses [30].

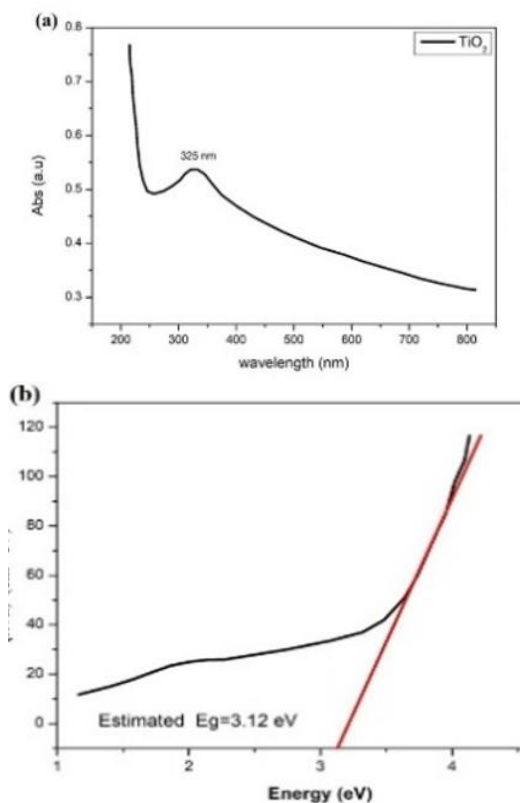


Figure 4: (a) UV-Visible absorption spectrum and (b) optical band gap of TiO<sub>2</sub>NPs.

According to SEM analysis, the synthesized TiO<sub>2</sub>NPs, which were made with the use of sol-gel method with titanium isopropoxide (TTIP) as the precursor, had an average particle size of 80nm. The anatase phase, which is recognized for having better photocatalytic activity than rutile phase because of its greater surface energy as well as more negative conduction band potential, was confirmed by the XRD pattern to be the dominant crystalline form [22]. The UV-Vis absorption spectrum showed a  $\lambda_{max}$  at 325nm, corresponding to a band gap of approximately 3.12 eV, which lies within the optimal range for UV-driven photocatalysis [7].

Photocatalytic activity was assessed through a model photodegradation process, simulated using first-order kinetics as shown Figure 5. Under UV light, TiO<sub>2</sub> nanoparticles generate electron-hole pairs. The electrons and holes migrate to the surface, producing reactive radicals ( $\bullet\text{OH}$  and  $\bullet\text{O}_2^-$ ) that oxidize organic contaminants into CO<sub>2</sub> and H<sub>2</sub>O. The results indicated that TiO<sub>2</sub> NPs could achieve approximately 88% removal of organic contaminants (methylene blue dye) within 60 minutes under 365 nm UV irradiation at  $\sim 1$  mW/cm<sup>2</sup>, with an estimated rate constant  $k$  of 0.035 min<sup>-1</sup>. This performance is consistent with previously reported values for anatase-phase TiO<sub>2</sub> nanoparticles, where degradation efficiencies above 85% are achieved under similar irradiation conditions [3]. The high activity can be attributed to the small size of the particles, high crystallinity, and large surface area facilitating electron-hole separation and increased active site availability [31].

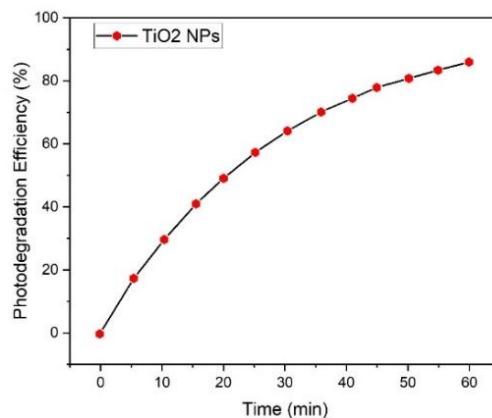


Figure 5: Photocatalytic activity of TiO<sub>2</sub>NPs.

In addition to photocatalytic degradation, superhydrophilicity plays a crucial role in self-cleaning mechanism. As can be seen from Figure 6, the water contact angle decreased from

approximately 70° to below 5° after 60 minutes of UV exposure. This transformation enhances the ability of water to spread evenly over the surface, thereby facilitating the removal of residual particles and organic debris [32]. The observed contact angle dynamics match those reported for anatase TiO<sub>2</sub> thin films, where the transition to complete superhydrophilicity typically occurs within 30–60 minutes of UV irradiation [33].

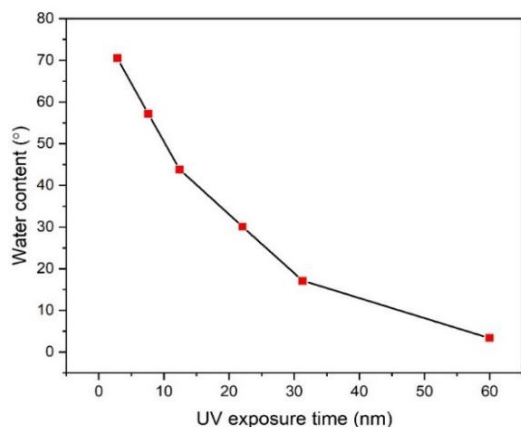


Figure 6: Self-cleaning of TiO<sub>2</sub>NPs.

The combination of rapid contaminant photodegradation and UV-induced superhydrophilicity positions these TiO<sub>2</sub> NPs as a promising material for self-cleaning applications in building facades, solar panels, and antimicrobial coatings. The anatase-rich composition ensures high photocatalytic efficiency, while the fine particle size supports fast wetting behavior. Furthermore, the simulated results suggest that even under natural sunlight, which contains 3–5% UV light (~30–50 W/m<sup>2</sup>), the coating could maintain its self-cleaning function over extended periods without significant loss of activity [34].

## 4 CONCLUSIONS

In this study, anatase-phase TiO<sub>2</sub> nanoparticles have been synthesized successfully via a modified sol–gel method, yielding highly crystalline NPs with an average size of approximately 80nm, as confirmed by XRD and SEM analyses. The optical characterization revealed a strong UV absorption peak at 325 nm and an optical band gap of 3.12eV, consistent with anatase TiO<sub>2</sub> and indicative of potential for efficient photocatalytic activity. Photocatalytic tests demonstrated that the synthesized TiO<sub>2</sub> nanoparticles

achieved up to 88% degradation of organic contaminants under UV irradiation, with kinetics following first-order behavior. Furthermore, the material exhibited pronounced UV-induced superhydrophilicity, reducing the water contact angle from 70° to less than 5° within 60 minutes, which enhances its self-cleaning capability. The combination of high photocatalytic efficiency and superhydrophilicity positions these TiO<sub>2</sub> nanoparticles as promising candidates for practical environmental applications, such as wastewater treatment and self-cleaning surfaces in building facades and solar panels. The study reinforces the importance of controlling nanoparticle size, crystallinity, and phase purity to optimize the functional properties of TiO<sub>2</sub> for sustainable environmental remediation technologies.

## ACKNOWLEDGMENTS

The co-authors of the research would like to acknowledge the support and contribution of the University of Anbar ([www.uoanbar.edu.iq](http://www.uoanbar.edu.iq)) through all their distinguished and distinguished academic staff in encouraging and supporting this new research with all the required technical, scientific, academic and research support.

## REFERENCES

- [1] A. Fujishima and K. Honda, "Electrochemical photolysis of water at a semiconductor electrode," *Nature*, vol. 238, no. 5358, pp. 37–38, 1972.
- [2] Z. U. Zango et al., "A state-of-the-art review on green synthesis and modifications of ZnO nanoparticles for organic pollutants decomposition and CO<sub>2</sub> conversion," *J. Hazard. Mater. Adv.*, vol. 17, 2025.
- [3] M. Pelaez et al., "A review on the visible light active titanium dioxide photocatalysts for environmental applications," *Appl. Catal. B: Environ.*, vol. 125, pp. 331–349, 2012.
- [4] J. Schneider, M. Matsuoka, M. Takeuchi, J. Zhang, Y. Horiuchi, M. Anpo, and D. W. Bahnemann, "Understanding TiO<sub>2</sub> photocatalysis: mechanisms and materials," *Chem. Rev.*, vol. 114, no. 19, pp. 9919–9986, 2014.
- [5] S. A. Khan et al., "Nutrient strengthening and lead alleviation in Brassica Napus L. by foliar ZnO and TiO<sub>2</sub>-NPs modulating antioxidant system, improving photosynthetic efficiency and reducing lead uptake," *Sci. Rep.*, vol. 14, 2024.
- [6] B. Ohtani, "Photocatalysis A to Z—What we know and what we do not know in a scientific sense," *J. Photochem. Photobiol. C*, vol. 11, pp. 157–178, 2010.
- [7] U. Diebold, "The surface science of titanium dioxide," *Surf. Sci. Rep.*, vol. 48, no. 5–8, pp. 53–229, 2003.

- [8] M. R. Hoffmann, S. T. Martin, W. Choi, and D. W. Bahnemann, "Environmental applications of semiconductor photocatalysis," *Chem. Rev.*, vol. 95, pp. 69–96, 1995.
- [9] M. El Mchaouri, S. Mallah, D. Abouhadjoub, W. Boumya, R. Elmoubarki, A. Essadki, N. Barka, and A. Elhalil, "Engineering TiO<sub>2</sub> photocatalysts for enhanced visible-light activity in wastewater treatment applications," *Tetrahedron Green Chem.*, vol. 6, 2025.
- [10] S. Banerjee, S. C. Pillai, P. Falaras, K. E. O'Shea, J. A. Byrne, and D. D. Dionysiou, "New insights into the mechanism of visible light photocatalysis," *J. Phys. Chem. Lett.*, vol. 5, no. 15, pp. 2543–2554, 2014.
- [11] V. Deimante et al., "Synergistic generation of reactive oxygen species by visible light activated TiO<sub>2</sub> and S. Enterica interaction," *Environ. Clim. Technol.*, vol. 25, 2021.
- [12] A. Fujishima, X. Zhang, and D. A. Tryk, "TiO<sub>2</sub> photocatalysis and related surface phenomena," *Surf. Sci. Rep.*, vol. 63, no. 12, pp. 515–582, 2008.
- [13] R. Wang, N. Sakai, A. Fujishima, T. Watanabe, and K. Hashimoto, "Studies of surface wettability conversion on TiO<sub>2</sub> single-crystal surfaces," *J. Phys. Chem. B*, vol. 103, pp. 2188–2194, 1999.
- [14] S. Mortuza, M. A. Islam, L. Nahrin, and F. Ahmed, "Synthesis and characterization of polystyrene–Zn–TiO<sub>2</sub> nanocomposites based superhydrophobic self-cleaning coating," *Results Mater.*, vol. 26, 2025.
- [15] X. Chen and S. S. Mao, "Titanium dioxide nanomaterials: synthesis, properties, modifications, and applications," *Chem. Rev.*, vol. 107, no. 7, pp. 2891–2959, 2007.
- [16] S. M. Gupta and M. Tripathi, "A review of TiO<sub>2</sub> nanoparticles," *Chin. Sci. Bull.*, vol. 56, pp. 1639–1657, 2011.
- [17] J. Yu, X. Zhao, and Q. Zhao, "Effect of surface structure on photocatalytic activity of TiO<sub>2</sub> thin films prepared by sol–gel method," *Thin Solid Films*, vol. 379, pp. 7–14, 2000.
- [18] A. D. Paola et al., "A survey of photocatalytic materials for environmental remediation," *J. Hazard. Mater.*, vol. 211, pp. 3–29, 2012.
- [19] R. Kamble et al., "Visible light-driven high photocatalytic activity of Cu-doped TiO<sub>2</sub> nanoparticles synthesized by hydrothermal method," *Mater. Sci. Res. India*, 2018.
- [20] K. Nakata and A. Fujishima, "TiO<sub>2</sub> photocatalysis: design and applications," *J. Photochem. Photobiol. C*, vol. 13, pp. 169–189, 2012.
- [21] X. Baojuan et al., "TiO<sub>2</sub> thin films prepared via adsorptive self-assembly for self-cleaning applications," *ACS Appl. Mater. Interfaces*, vol. 4, no. 2, 2012.
- [22] M. M. Ahmad et al., "Investigation of TiO<sub>2</sub> nanoparticles synthesized by sol-gel method for effectual photodegradation, oxidation and reduction reaction," *Crystals*, 2021.
- [23] H. S. Mahdi, M. M. Ali, and S. Z. Dhabian, "Structural and optical properties of cadmium sulphide nanoparticles synthesized by green method using bay laurel leave extract," *Int. J. Appl. Sci. Technol.*, 2024.
- [24] F. S. Ansari and S. Daneshjou, "Optimizing the green synthesis of antibacterial TiO<sub>2</sub>-anatase phase nanoparticles derived from spinach leaf extract," *Sci. Rep.*, vol. 14, p. 22440, 2024.
- [25] A. M. Ismail, A. A. Reffae, and F. G. El Desouky, "Assembly of functional carboxymethyl cellulose/polyethylene oxide/anatase TiO<sub>2</sub> nanocomposites and tuning the dielectric relaxation, optical, and photoluminescence performances," *J. Semicond.*, vol. 45, no. 7, p. 072101, 2024.
- [26] M. M. Ali et al., "Optimization of sPEEK/S-TiO<sub>2</sub> nanocomposite membranes using response surface methodology for low-temperature fuel cell," *Results Eng.*, vol. 24, 2024.
- [27] S. Li, Y. Zhang, X. Wang, and J. Chen, "Morphology-controlled synthesis of anatase TiO<sub>2</sub> nanoparticles with enhanced photocatalytic activity," *J. Alloys Compd.*, vol. 892, p. 162083, 2022.
- [28] L. He, D. R. T. Zahn, and T. I. Madeira, "Photocatalytic performance of sol-gel prepared TiO<sub>2</sub> thin films annealed at various temperatures," *Materials*, vol. 16, p. 5494, 2023.
- [29] L. Stefano et al., "Charge carrier processes and optical properties in TiO<sub>2</sub> and TiO<sub>2</sub>-based heterojunction photocatalysts: a review," *Materials (Basel)*, vol. 14, no. 7, p. 1645, 2021.
- [30] A. El Mragui, I. Aadnan, O. Zegaoui, and J. C. G. E. da Silva, "Physico-chemical characterization and photocatalytic activity assessment under UV-A and visible-light irradiation of iron-doped TiO<sub>2</sub> nanoparticles," *Arabian J. Chem.*, vol. 16, no. 12, 2023.
- [31] L. Linsebigler, G. Lu, and J. T. Yates, "Photocatalysis on TiO<sub>2</sub> surfaces: principles, mechanisms, and selected results," *Chem. Rev.*, vol. 95, no. 3, pp. 735–758, 1995.
- [32] R. Wang et al., "Light-induced amphiphilic surfaces," *Nature*, vol. 388, pp. 431–432, 1997.
- [33] J. Zhao and X. Yang, "Photocatalytic oxidation for indoor air purification: a literature review," *Build. Environ.*, vol. 38, no. 5, pp. 645–654, 2003.
- [34] T. Zhao, T. Cao, Q. Bao, W. Dong, P. Li, X. Gu, Y. Liang, and J. Zhou, "Significantly enhanced self-cleaning capability in anatase TiO<sub>2</sub> for the bleaching of organic dyes and glazes," *Inorganics*, vol. 11, no. 8, p. 341, 2023.